THE ELECTRON-PROTON EFFECTS IN INTENSE PROTON BUNCHES

BNL/NSNS TECHNICAL NOTE
NO. 008

A. G. Ruggiero and M. Blaskiewicz

January 15, 1997

ALTERNATING GRADIENT SYNCHROTRON DEPARTMENT
BROOKHAVEN NATIONAL LABORATORY
UPTON, NEW YORK 11973

The Electron-Proton Effects in Intense Proton Bunches

A. G. Ruggiero and M. Blaskiewicz

Brookhaven National Laboratory

December 5, 1996

Background

It has been speculated that the intensity limitation observed in the Los Alamos Proton Storage Ring (PSR) is caused by a coherent instability [1] induced by the presence of pockets of electrons generated by scattering with the molecules of the vacuum residual gas. This is commonly referred to as the "e-p instability". A similar instability has been observed in electron storage rings [2] where, this time, the effect is induced by the positive ions produced by ionization of the residual gas. A theoretical framework does exist to explain the ion-induced instability [3], and the experimental observations as well as the cures adopted are in fairly good agreement with the theoretical predictions. Cures generally include: vacuum improvement, careful design of bunch length and spacing, and installation of clearing electrodes to sweep the ions away from the regions where they have tendency to accumulate.

The e-p instability of proton beams has been directly observed only in the old Intersecting Storage Rings in CERN [4]. Here, nevertheless, the proton beam was very intense (few tens of amperes), and completely debunched, that resulted in a deep and continuous transverse barrier from which electrons could hardly escape. Clearing electrodes and vacuum improvement have been the major cures to cope with the instability in the ISR. This instability actually was not the major current limitation in the ISR, which was due to the so-called "brick-wall effect", a beam-wall coupling impedance induced instability. Beyond this, the e-p instability has never been observed in other proton accelerators, where usually the beam is bunched. That the e-p instability may cause, directly or indirectly, the intensity limitation observed in the PSR is still a speculation that remains to be demonstrated.

A theoretical explanation of the e-p instability of course does exist [5], and is similar to the one developed for the ion-induced instability in electron storage rings, with the exception that the role of the positive ions is replaced by that of the electrons. One major difference, which partially explains the different behavior of proton and electron bunched beams, is the difference in mass and initial velocity of the ions and electrons produced during the vacuum gas ionization process. The electrons have the tendency to drift quickly away from the beam, whereas the positive ions stay in the vacuum chamber for a considerably longer period of time, and their motion is clearly affected by the repetitive passage of the beam bunches.

Relevance to the NSNS Accumulator Ring

Considering the large beam power (1 - 2 MW) involved in the NSNS Accumulator Ring [6], and the consequences caused by even a small amount of beam loss, we need to carefully assess the effects of electrons that may be generated in the vacuum chamber. At this purpose we shall draw from the experimental observations available from the PSR, and work with the theoretical model that has been developed consequently. Furthermore, we shall expand this theoretical understanding with a more complete and refined analysis of our own.

Of course, a major difference is that the PSR does already exist, since it was built years ago with the wisdom and the knowledge of that time. It is clear that the PSR, at the moment, suffers of other serious limitations, for instance: large space-charge depression, proximity to an integer resonance of the operating tune, poor vacuum conditions, insufficient rf compressing system, no safety margin between ring physical acceptance and beam emittance, and no clearing electrodes installed in the system. It has already been judged that all these limitations to the operation of the PSR do not help to cope with, or even to learn more about the observed intensity limitation and that the situation is too constrained to devise immediate cures. Indeed an upgrade program of the PSR has already been proposed [7], which requires some financial burden and time, to eliminate at least part of the present constraints.

Obviously, the design of the NSNS Accumulator Ring has to draw from the past experience, and to guarantee that all measures for a good operation are taken into account, namely: control of the space-charge tune-shift, capability to tune the beam away from major low-order resonances, choice of the operating tunes away from integer and half-integer resonances, good vacuum system in the 10^{-9} to 10^{-10} mmHg range, good and controllable rf bunching system, plenty of clearance between physical acceptance and beam emittance of at least a factor of four, and, if it is needed, installation of clearing electrodes, or, otherwise, understanding and control of the sources of electrons in the ring.

It remains a positive and encouraging fact that the e-p instability has not been observed in other accelerators of bunched proton beams, aside from the PSR, which, after all, after a more careful examination, may reveal a different mechanism which causes the intensity limitations. We all would be interested in the discovery of such a mechanism which indeed, eventually, should be taken into account in the design of the NSNS Accumulator Ring. But for the time being, because of the uncertainty, we shall have to assume the e-p instability model, deferring any other conclusion to the time when the PSR staff, alone or in collaboration with other laboratories, will have solved the PSR problem more directly.

Sources of Electrons in the NSNS Accumulator Ring

Electrons may be generated in a variety of ways which are listed and explained below.

Negative ions traverse the stripping foil during injection. Here two electrons are generated for each negative ion entering the ring; thus the rate of electron production is twice the primary beam intensity. The average power associated to the electrons is 2.2 kW, corresponding to 1 GeV pri-

mary beam with an average power of 2 MW. The electrons are produced forward, with the same velocity distribution of the primary beam, and a central energy value of 0.544 MeV. There may be a spreading of transverse and longitudinal momenta caused by multiple Coulomb scattering with the foil and the space charge forces with the other electrons and the proton beam itself. Leaving the foil, the electrons will drift forward and enter a 2.5 kG bending magnet [8], which is part of the horizontal set-up for the beam multiturn injection. The trajectory in the magnet is a semicircle of 10 cm diameter, at the end of which they are collected by a water-cooled copper and graphite collector, disposed parallel to the motion of the incoming beam. The system requires some careful engineering design, but it is feasible, and care should be applied to guarantee that all electrons are indeed collected and swept away from the beam.

The second mechanism of electron production is the loss of protons on the vacuum chamber wall. If a proton hits the wall, electrons may be desorbed, which in turn may hit the wall again, and desorb more electrons through a process known as "multipactoring". The effect of this mechanism is controlled by minimizing the loss of the protons to the wall. The design requirement for this purpose is a total loss not exceeding 10^{-4} of the total proton beam intensity, which is achieved by allowing a factor four between physical acceptance and full beam emittance all around the ring, and by insertion of collimators/scrapers in conveniently chosen locations to intercept the beam halo. Moreover, special care is given to the design of the injection region to guarantee capture and dump of those negative ions which have not successfully stripped [8]. Also, the vacuum chamber will be made of treated, or otherwise coated stainless steel, and not of aluminum, to eliminate or considerably reduce electron desorbtion and multipactoring.

Unfortunately, among other things, collimators/scrapers will also generate electrons. Fortunately, preliminary design and calculations [9] have shown that only 10^{-4} electrons are produced in their proximity, for each circulating proton. The energy of these electrons is very high, in the MeV range, and are therefore capable to reach immediately the vacuum chamber between passages of the beam bunch. Of course, the vacuum chamber material, in the proximity of the collimators, is to be of property such not to create desorbtion problems that may be caused by these energetic electrons.

Probably the source of electrons with more serious consequences to the beam stability is the vacuum residual gas. For economic reasons, and simplicity, we have opted for an average pressure of 10^{-9} Torr equivalent nitrogen. If desired and needed, a more expensive system capable of 10^{-10} Torr can also be built. The vacuum chamber of the NSNS Accumulator Ring has a large aperture, that is an average diameter $2b = 20$ cm all the way around, which should make the operation of the vacuum system easier. In the following, we shall examine the effects of the electrons generated by the ionization of the residual gas on the beam stability. The positive ions which are also produced during the ionization process, because of the same sign of the electric charge as the protons, are pushed away from the proton beam toward the wall of the vacuum chamber where they are expected to be absorbed. Of course, this is also a point of concern which will affect the choice of the vacuum chamber material to carefully eliminate desorbtion of secondary electrons.

Electron Production by Residual Gas Ionization

We shall estimate next the production rate of electrons during the ionization process of the vacuum residual gas. For this purpose, and for the following calculations, we have summarized the general parameters of the NSNS Accumulator Ring in Table 1.

Table 1: Parameters of the NSNS Accumulator Ring

Beam Kinetic Energy	1.0 GeV
Magnetic Rigidity	5.657 T m
β	0.875
γ	2.066
Beam Average Power	2.0 MW
Total Number of Protons, N_T	2.08×10^{14}
No. of Injected Turns	1250
Revolution Period, T_0	795 ns
Injection Period, T_{inj}	1.0 ms
Bunch Length, T	515 ns
Beam Gap, τ	280 ns
Beam Average Radius, a	50 mm
Vacuum Chamber Radius, b	100 mm
Circumference, $2\pi R$	209 m
Betatron Tune (H and V)	3.8
Average Vacuum Pressure	10^{-9} Torr (equiv. N_2)

We shall assume here average vacuum values, waiting that better defined gas composition and corresponding ionization cross-sections are made available after the design of the vacuum system. We have assumed an average vacuum pressure, nitrogen equivalent, of 10^{-9} Torr. This corresponds to a residual gas density

$$n = 6 \times 10^7 \text{ atoms / cm}^3 \text{ at normal conditions.} \quad (1)$$

The expected average ionization cross-section

$$\sigma_i = 2.5 \times 10^{-18} \text{ cm}^2 \quad (2)$$

but could easily vary by a factor of 3.

The rate of electron production is then given by

$$d\,n_e / dt = \beta\, c\, n\, \sigma_i\, N(t)$$

$$= \beta\, c\, n\, \sigma_i\, N_r\, t = 1 / \tau_{prod} \qquad (3)$$

where N(t) is the number of protons which varies during injection according to $N(t) = N_r\, t$, with $N_r = N_T / T_{inj} = 2.04 \times 10^{17}$ protons / s. The production time τ_{prod} is plotted in Figure 1 during the injection process.

We assume that, at the end of the injection process, the beam has already been longitudinally compressed and that it is immediately extracted to the target area for neutron production. Thus, we shall be concerned about the beam stability only during the period of time T_{inj}. Integration of (3) gives

$$\chi = n_e / N_T = 1/2\ \beta\, c\, n\, \sigma_i\, T_{inj}$$

$$= 0.002 \quad \text{electrons / proton} \qquad (4)$$

that is a beam charge neutralization $\chi = 0.2$ %, which is independent of the final beam intensity N_T. This figure is about an order of magnitude lower than the one that was indirectly estimated for the PSR ring. The difference, obviously, is due to the different vacuum pressure conditions.

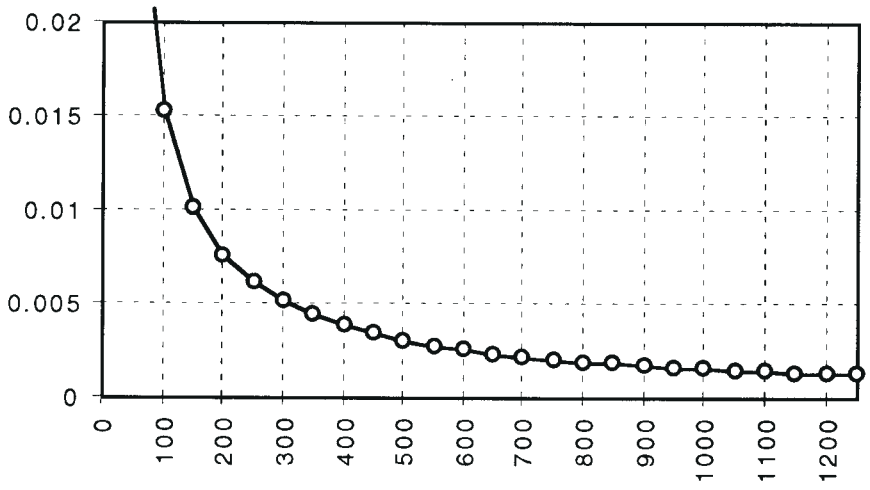

Figure 1. Production Time τ_{prod} in picoseconds versus the number of injected turns

Motion of the Electrons

To understand the dynamics of the electrons and, thus, of the protons, it is necessary to have an idea of the motion of the electrons in the various components that make up the Accumulator Ring, namely: drifts, dipole magnets and quadrupole magnets. The motion has to be calculated

under the presence of both the external forces, which are in the bending and focussing elements of the ring, and the space-charge forces created by the proton beam. For this purpose, we shall assume that the proton beam bunch is a cylinder with dimensions given in Table 1, with transverse and longitudinal uniform charge distribution. There is a single proton beam bunch.

At any particular location of the ring, electrons are produced at random transverse position within the beam bunch, with a velocity distribution [10] which spans over an energy range of few eV. This is considerably less than the difference in electrostatic potential between the center and edge of the beam of several kVolt. Of course, space charge forces are important only when the electrons are within the proton bunch; in the beam gap region they are subject only to the effects of the external forces. It is then important to consider the motion within the proton bunch and outside separately. The motion will acquire a periodic behavior which is due to the periodic passage of the proton bunch. The length of the periodicity is T_0, the revolution period in the ring, which is broken down in two steps, one of length T which equals the length of the proton bunch, and the other of length τ, equal to the length of the beam gap. As the proton bunch leaves the location where the electrons are produced, they receive a longitudinal kick which increases their energy and longitudinal velocity in the direction of the bunch motion. When the other end of the bunch enters the same location, electrons will receive a similar kick but in the opposite direction, cancelling therefore the previous one. It results that electrons will all together drift in the same direction of the bunch motion during the period of time τ which corresponds to the beam gap.

Motion in the Drifts

The equations of motion are very simple:

In the beam gap region

$$d^2x / dt^2 = d^2y / dt^2 = d^2z / dt^2 = 0 \qquad (5)$$

where x and y denote the horizontal and vertical directions of motion, and z the longitudinal direction, along the main motion of the proton beam. In the region where the beam bunch is present

$$d^2x / dt^2 + \Omega_e^2 x = 0 \qquad (6a)$$

$$d^2y / dt^2 + \Omega_e^2 y = 0 \qquad (6b)$$

$$d^2z / dt^2 = 0 \qquad (6c)$$

except, as we have noted, that there are compensating longitudinal kicks the electrons receive at the transition between the two regions.

Thus in the beam gap region the motion is a pure drift, where the electrons have an opportunity to leave the beam and reach the vacuum chamber wall. Since the vacuum chamber is about 10 cm away from the beam axis, and the beam gap lasts 280 ns, it will require a transverse velocity

$v_e = 0.36 \times 10^6$ m / s to escape, that is $\beta_e \sim 0.0012$, which corresponds to an energy of about 0.36 eV. It is not clear how many electrons will be produced with an energy less than this, but only a very small fraction of the total is expected [10]. Thus most of the electrons produced by the residual gas ionization, in the drift regions, will be able to escape the beam, and be absorbed by the vacuum chamber wall. It derives that the neutralization coefficient χ given by equation (4) is expected to be considerably lower by several orders of magnitude.

In the presence of the proton bunch, the bouncing angular frequency

$$\Omega_e^2 = 2 N(t) r_e c^2 / a^2 L \tag{7}$$

where $r_e = 2.82 \times 10^{-15}$ m, and $L = \beta cT = 135$ m is the bunch physical length. The bouncing frequency $\Omega_e / 2\pi$ is plotted in Figure 2 during the injection process. At the end of injection $\Omega_e / 2\pi$ = 90 MHz, and it is about few MHz already with the first turn injected. The bouncing frequency is considerably higher then any other frequency which characterizes the beam motion. Electrons perform several transverse oscillations during the passage of the proton bunch.

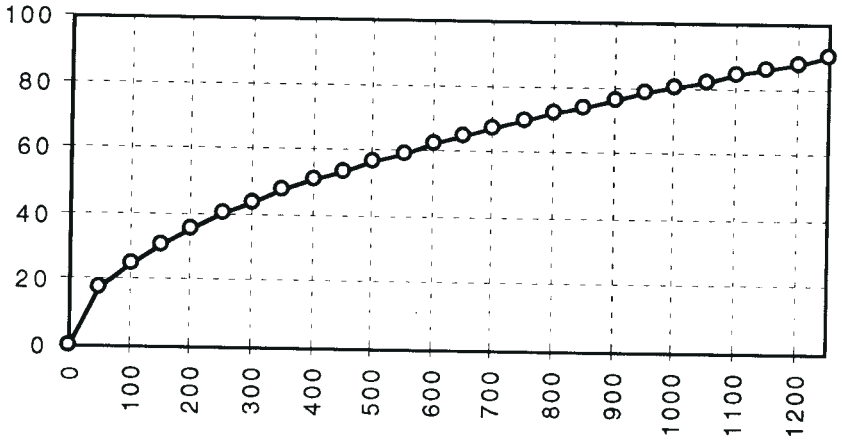

Figure 2. The electron Bouncing Frequency $\Omega_e / 2\pi$ (MHz) versus the number of injected turns

If we take an electron transverse velocity of $v_e = 1 \times 10^6$ m/s, the amplitude of the transverse oscillations is only a couple of millimeters at the end of the injection, but several centimeters at the beginning of injection. Equations (6a and b) are really valid only as long as the electron motion is confined radially within the proton bunch. If the electron happens to be outside, the equations of motion then are

$$d^2x / dt^2 + \Omega_e^2 a^2 / x = 0 \tag{8a}$$

$$d^2y / dt^2 + \Omega_e^2 a^2 / y = 0 \tag{8b}$$

which are not of easy solution. The following applies only in the case the electron displacement from the proton beam axis is less than the radius of the proton beam. Each electron receives a periodic transverse attractive kick when is traversing the proton bunch, followed by a drift

between two consecutive passages. The system of Equations (5a and b) and (6a and b) can be solved with the matrix method. The transfer matrix over one period, which includes one beam gap and one beam bunch, is

$$M = \begin{vmatrix} \cos\phi - \Omega_e \tau \sin\phi & (1/\Omega_e)\sin\phi + \tau\cos\phi \\ -\Omega_e \sin\phi & \cos\phi \end{vmatrix} \quad (9)$$

where $\alpha = \Omega_e \tau / 2$ and $\phi = \Omega_e T$. The stability of motion, that is of electron trapping, is determined by the condition $|\mathrm{Tr}\, M| < 2$, that is

$$|\cos\phi - \alpha \sin\phi| < 1 \quad (10)$$

The absolute value of half of the Trace of M is plotted versus the number of injected turns in Figures 3 to 6 for different values of the beam gap length τ.

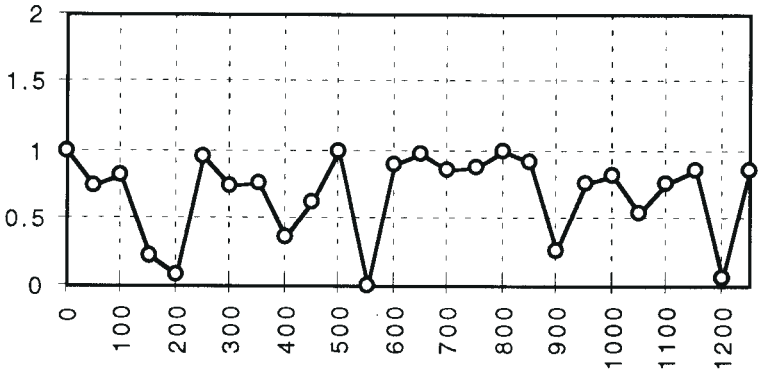

Figure 3. 1/2 | Tr M | versus the Number of Injected Turns for debunched beam, $\tau = 0$

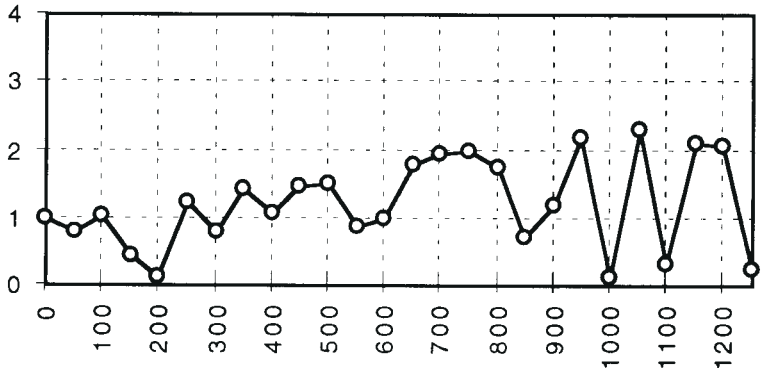

Figure 4. 1/2 | Tr M | versus the Number of Injected Turns for $\tau = 10$ ns

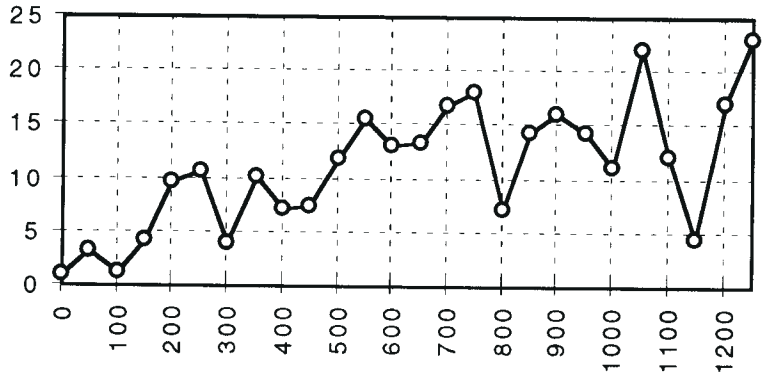

Figure 5. 1/2 | Tr M | versus the Number of Injected Turns for $\tau = 100$ ns

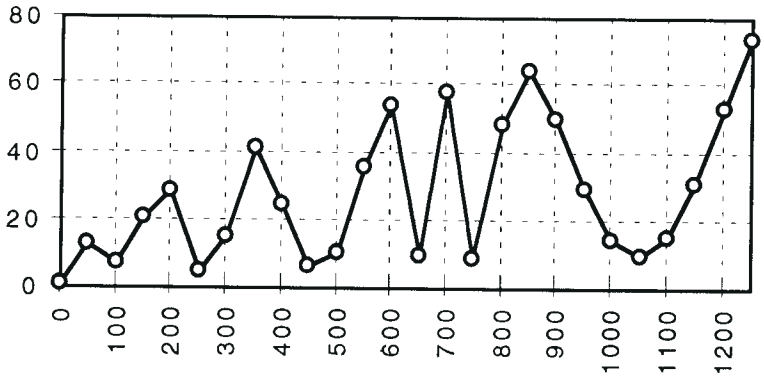

Figure 6. 1/2 | Tr M | versus the Number of Injected Turns for $\tau = 280$ ns

It is seen that when the beam is completely debunched, that is $\tau = 0$, the motion is always stable and the electrons are trapped, in agreement with the ISR observations. But already with a beam gap of only $\tau = 10$ ns, as the beam intensity increases during injection, the motion becomes unstable. Condition (10) for electron trapping is not satisfied for $\tau > 100$ ns during the entire injection process, and as a consequence the electrons are supposed to leave the beam bunch and escape to the wall, whatever is their initial velocity. Of course as the electron leaves the beam, the equations of motion (6a and b) are not valid, and the equations (8a and b) apply. But our derivation gives a good indication for the condition of electron trapping. Actually, one can also estimate the time that is required for the electrons to leave the beam and reach the wall, since that is also given by the trace itself of the transfer matrix if we write, when the motion is unstable,

$$| \cos \phi - \alpha \sin \phi | = \cosh \mu \qquad (11)$$

Denoting with $f_0 = 1/ T_0$ the revolution frequency, $\mu f_0 = 1 / \tau_{esc}$ is the escape rate which is plotted in Figure 7 during the injection process. The actual number of electrons present in the vacuum chamber in a drift section is then given by the balance of the escape rate and the production rate,

shown in Figure 1, that is when

$$d\, n_e / dt \;=\; \beta\, c\, n\, \sigma_i\, N(t) \;-\; n_e / \tau_{esc} \;=\; 0 \qquad (12)$$

At the end of the injection process we estimate that 1.3×10^8 electrons remain in a drift section, which yields a neutralization coefficient $\chi = 6.3 \times 10^{-7}$.

Figure 7. The electron escape time τ_{esc} (ns) vs. the number of injected turns, in a drift, for a bunch gap $\tau = 280$ ns

Effect of a beam leakage in the bunch gap

It has been speculated [1] that the ep instability observed in the PSR ring could be caused by an amount of proton beam which leaked in the bunch gap. Indeed, otherwise, with a completely clear beam gap, one could not explain the effect on the proton bunch.

In the NSNS Accumulator Ring the design calls for the provision of an rf system which compresses the beam in a single bunch during the injection process [11]. The rf system can be made of a single harmonic, a double harmonic, or a bucket barrier. The system will guarantee a gap completely clear of beam to a level of 10^{-5} of the total proton intensity, with a longitudinal extension of 280 ns [12]. This is also required for a clean beam extraction of a single turn by a fast kicker magnet. A 50 - 80 % safety margin does exist between the bucket area provided by the rf system and the total bunch area which is expected to be around 10 eV-s. No proton leakage is thus expected to occur toward the bunch gap in the NSNS Accumulator Ring. Nevertheless, we shall assume here that a small fraction η of the proton beam could be present in the gap. The transfer matrix (9) will then be modified accordingly to yield a new stability condition

$$\left| \; 2 \cos \phi_B \cos \phi_G \;-\; \left(\Omega_G / \Omega_B \;+\; \Omega_B / \Omega_G \right) \sin \phi_B \sin \phi_G \; \right| \;<\; 2 \qquad (13)$$

where

$$\Omega_B^2 = \Omega_e^2 (1 - \eta) \tag{14a}$$

$$\Omega_G^2 = \Omega_e^2 \eta \tag{14b}$$

and

$$\phi_B = \phi (1 - \eta)^{1/2} \tag{15a}$$

$$\phi_G = \phi \eta^{1/2} \tag{15b}$$

The absolute value of half the trace of the new transfer matrix is plotted in Figures 8 to 11, for a beam gap of $\tau = 280$ ns, and for various values of the beam fraction η in the bunch gap.

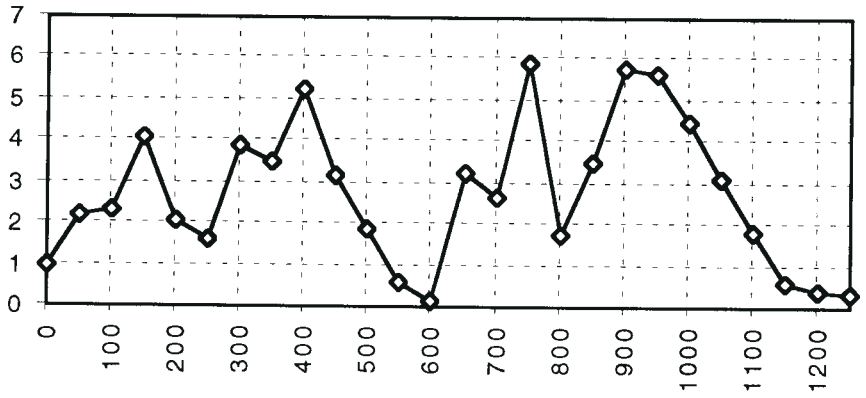

Figure 8. 1/2 | Tr M | versus the Number of Injected Turns for $\tau = 280$ ns and $\eta = 1\%$

It is seen that already with a 1% of the proton beam leaked in the bunch gap, stability and instability conditions alternate during the injection process. For larger value of η, the chances of electron trapping increases considerably. It is thus important that the bunching process will exclude protons to penetrate the gap at a rate larger than 0.1% of the total proton intensity, which case is shown in Figure 12.

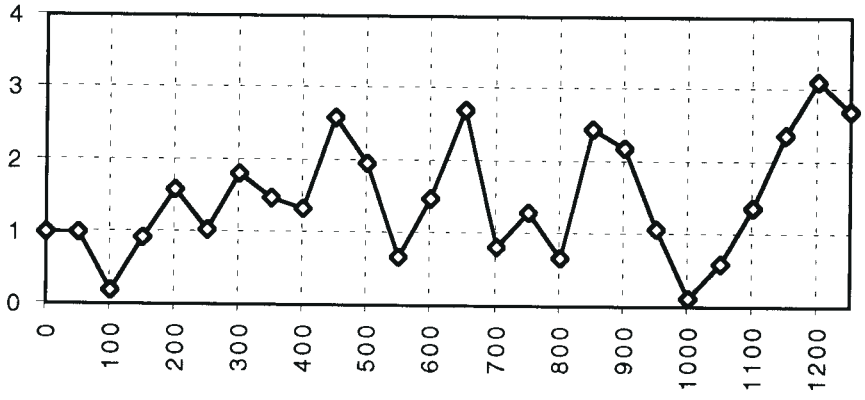

Figure 9. 1/2 | Tr M | versus the Number of Injected Turns for $\tau = 280$ ns and $\eta = 5\%$

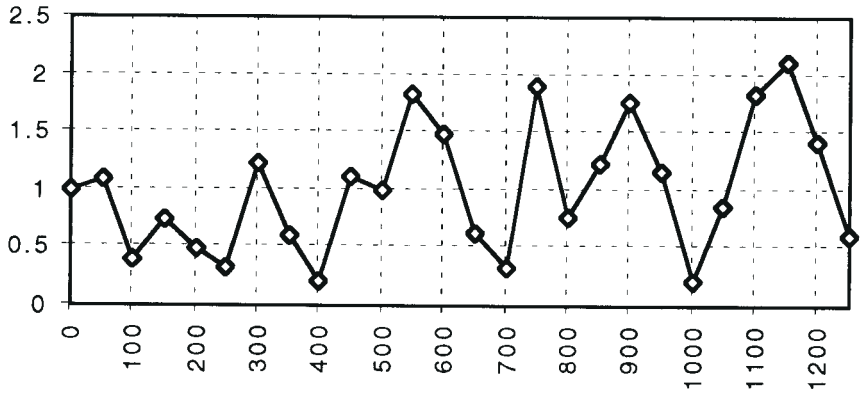

Figure 10. 1/2 | Tr M | versus the Number of Injected Turns for $\tau = 280$ ns and $\eta = 10\%$

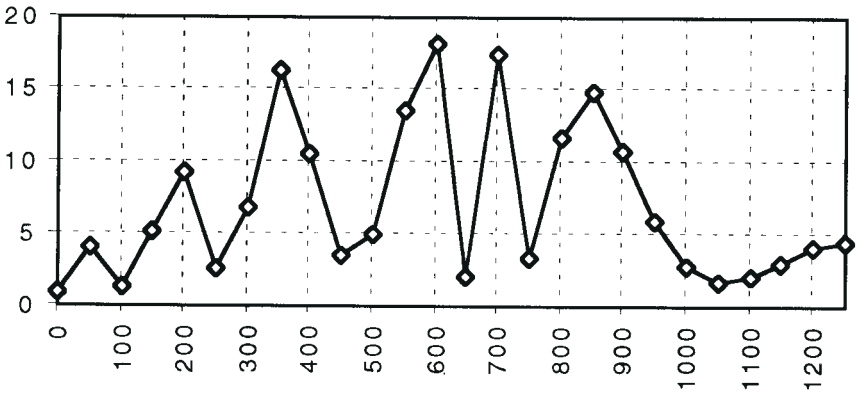

Figure 11. 1/2 | Tr M | versus the Number of Injected Turns for $\tau = 280$ ns and $\eta = 0.1\%$

Longitudinal Drift of the Electrons

As it was explained earlier, an electron receives longitudinal kicks when leaving and entering the proton bunch. The velocity change which accompanies the kick is given by

$$\Delta v_e = N(t)\, c\, e^2\, Z_{sc} / 2\pi\, m_e\, c^2\, \beta\, T \qquad (16)$$

where m_e is the electron mass, and the longitudinal space charge impedance

$$Z_{sc} = (377 \text{ ohm})\,(\,1 + 2 \log b/a\,) / 2\,\beta^2\,\gamma^2 \sim 140 \text{ ohm} \qquad (17)$$

At the end of injection, $\Delta v_e = 1 \times 10^6$ m/s which scales linearly with the proton beam intensity. This corresponds to an energy kick of about 2.5 eV. Thus, when produced, the electron has an initial velocity which increases when the leaving the proton bunch by Δv_e, and decreases by the same amount when entering the bunch again. Thus there is no longitudinal trapping of the elec-

trons, but a longitudinal drift in the direction of the proton beam motion. Every turn the electrons drift 27 cm in the same direction. This conclusion applies, of course, only to the drift sections.

Motion in the Bending Magnets

To evaluate the motion of the electrons in a dipole magnet, one has to modify equations (5), (6a to c) or (8a to b) to include the contribution from the dipole field. Within the bunch gap the equations of motion are

$$d^2x / dt^2 = - \Omega_L \, dz / dt \tag{18a}$$

$$d^2y / dt^2 = 0 \tag{18b}$$

$$d^2z / dt^2 = \Omega_L \, dx / dt \tag{18c}$$

where

$$\Omega_L = e B / m_e c \tag{19}$$

is the angular Larmor frequency with B the strength of the bending field. In the presence of the proton bunch, the equations are

$$d^2x / dt^2 + \Omega_e^2 x = - \Omega_L \, dz / dt \tag{20a}$$

$$d^2y / dt^2 + \Omega_e^2 y = 0 \tag{20b}$$

$$d^2z / dt^2 = \Omega_L \, dx / dt \tag{20c}$$

assuming that the electron is confined transversely within the dimension of the proton bunch, or, otherwise,

$$d^2x / dt^2 + \Omega_e^2 a^2 / x = - \Omega_L \, dz / dt \tag{21a}$$

$$d^2y / dt^2 + \Omega_e^2 a^2 / y = 0 \tag{21b}$$

$$d^2z / dt^2 = \Omega_L \, dx / dt \tag{21c}$$

Thus the vertical motion remains unchanged as in the drift sections, with the same consequences that have been described earlier. The horizontal and longitudinal components of the motion are now coupled to each other through the bending field. The motion on the horizontal plane is dominated by a precession movement at the Larmor frequency. In the NSNS Accumulator Ring, B = 1 Tesla and Ω_L = 165 GHz, which is very high indeed. The corresponding Larmor radius ρ_L = 6 μm for an electron of 2.5 eV kinetic energy. The most important result, nonetheless, is that the motion of the electrons in a dipole magnet is unbounded in the vertical direction, though they are trapped on the horizontal plane without any longitudinal drift. Electrons have still

the ability to escape the proton bunch vertically at the same rate as estimated for the case of the drift. The neutralization coefficient is thus expected to be small, as it was estimated for the drift sections.

We derive the following picture. Electrons that are produced in a drift are not trapped transversely, and have tendency to leave the beam at fast speed, both horizontally and vertically. Longitudinally, they drift toward the dipole magnets where are eventually trapped on the horizontal plane by the Larmor precession frequency. But they would still escape vertically. The same applies to those electrons that are produced in a dipole magnet, except that they do not drift longitudinally.

Motion in the Quadrupole Magnets

All the components of motion are now coupled to each other by the quadrupole gradient G. Moreover the equations of motion are now nonlinear and difficult to solve exactly. In the interval of the beam gap, only the contribution of the quadrupole field enters the equations:

$$d^2x / dt^2 = - (e G / m_e c) x \, dz / dt \quad (22a)$$

$$d^2y / dt^2 = (e G / m_e c) y \, dz / dt \quad (22b)$$

$$d^2z / dt^2 = (e G / m_e c) (x \, dx / dt - y \, dy / dt) \quad (22c)$$

During the traversal of the proton bunch these equations are modified to include the interaction with the proton beam:

$$d^2x / dt^2 + \Omega_e^2 x = - (e G / m_e c) x \, dz / dt \quad (23a)$$

$$d^2y / dt^2 + \Omega_e^2 y = (e G / m_e c) y \, dz / dt \quad (23b)$$

$$d^2z / dt^2 = (e G / m_e c) (x \, dx / dt - y \, dy / dt) \quad (23c)$$

As in the drift and in the dipole cases, also here, of course, the electron receives longitudinal kicks when leaving and entering the proton bunch.

Equations (22a to c) can be partially integrated to show that

$$v_e^2 = (dx / dt)^2 + (dy / dt)^2 + (dz / dt)^2 \quad (24)$$

is a constant of motion. Indeed the motion of a charged particle ina purely magnetic field does not alter its energy. It is thus sufficient to solve the system (22a and b) with dz/dt derived from (24).

The exact integration of the equations of motion can only be tried numerically. Here we shall assume that the longitudinal velocity $dz/dt = v_z$ of the electrons is essentially constant. With this assumption then the equations can be solved exactly. They become, in the beam gap interval

$$d^2x / dt^2 + \Omega_Q^2 x = 0 \quad (25a)$$

$$d^2y / dt^2 - \Omega_Q^2 y = 0 \quad (25b)$$

and during the traversal of the proton bunch

$$d^2x / dt^2 + (\Omega_e^2 + \Omega_Q^2) x = 0 \quad (26a)$$

$$d^2y / dt^2 + (\Omega_e^2 - \Omega_Q^2) y = 0 \quad (26b)$$

where

$$\Omega_Q^2 = e G v_z / m_e c \quad (27)$$

Thus, we have the equivalent of an external restoring force which alternates between two values. The analysis of this motion is also equivalent to the one already exposed for the case of presence of protons in the beam gap, and we can estimate the stability of the motion with the same method. A major difference is that the restoring force due to the quadrupole field has opposite sign in the two transverse plane of motion, has shown in the equations above. Moreover, the quadrupole gradient changes periodically from magnet to magnet; that is, Ω_Q^2 can be positive and negative depending on the sign of G, whereas Ω_e^2 is always positive. In the following we shall assume that v_z is positive and essentially given by the longitudinal kicks.

In the NSNS Accumulator Ring the gradient G = 0.21 kG/cm in the QF quadrupoles, and G = 0.24 kG/cm in the QD quadrupoles. Below we shall take the larger of these values. Figure 12 plots the two frequencies Ω_e and Ω_Q versus the number of injected turns. Positive values of G and v_z are assumed. The longitudinal velocity is calculated from the longitudinal kicks given during the transition of a bunch gap. It is seen that the two frequencies have about the same value, except that during the second half of the injection it appears that $\Omega_Q > \Omega_e$.

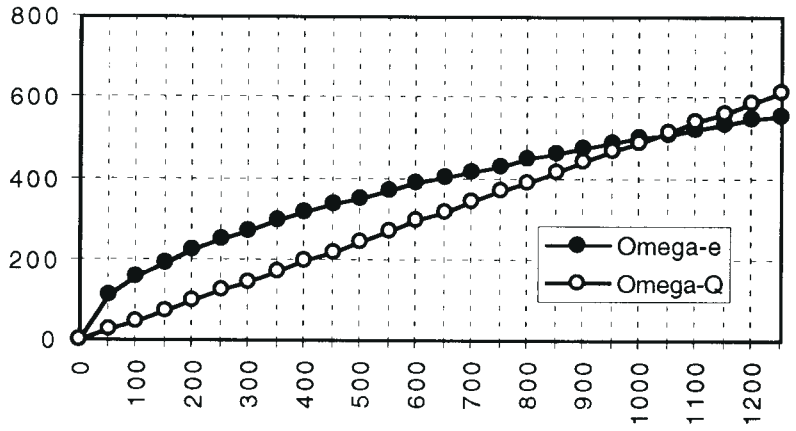

Figure 12. Ω_e and Ω_Q versus the number of injected turns.

Figures 13 and 14 are the plots of half of | Tr M | for G > 0 and G < 0 respectively. It is seen that whereas the motion of the electrons are stable and therefore are captured for the case G > 0, in the opposite case with G < 0 the electrons will escape at a very fast rate. This, of course, is not sufficient to infer that there are absolutely no problems with electrons being captured in the quadrupole magnets. It is obvious that one needs to integrate the system of equations (22 and 23) numerically. Determining the entire solution, though, may take considerable amount of time and effort.

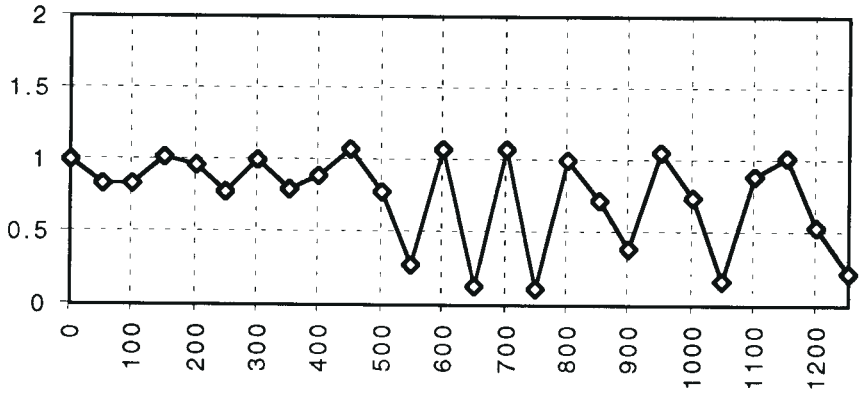

Figure 13. 1/2 | Tr M | in the Quadrupole magnets for G > 0

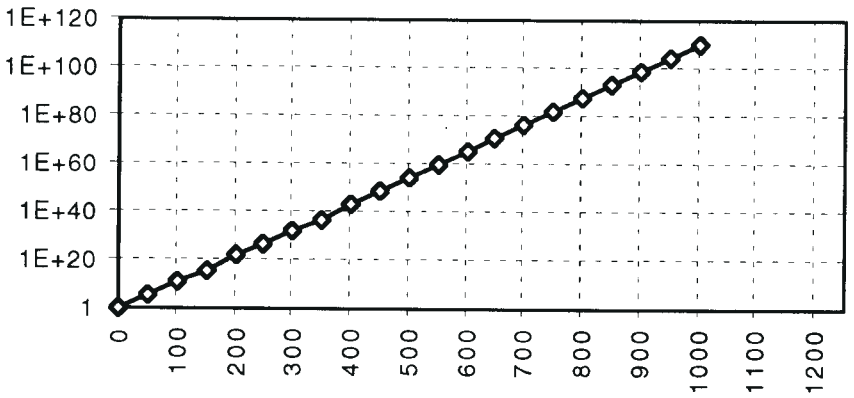

Figure 14. 1/2 | Tr M | in the Quadrupole magnets for G < 0

Clearing Electrodes

As we have seen, electrons have tendency to drift longitudinally from drift and quadrupole sections until they reach dipole magnets where they are trapped in the horizontal plane, though they can still escape vertically. Thus it may be convenient to place clearing electrodes at the upstream end of the dipole magnets to sweep whatever electrons have been accumulating there. The typical longitudinal separation of the electrodes is about 5 meter. As we have seen, electrons will move about 27 cm every revolution, and they will need at most 20 revolutions to travel toward a clearing electrode; that is a time interval τ_{ce} = 15 μs. The number of the electrons at the equilib-

rium can be determined from

$$d\, n_e / dt \;=\; \beta\, c\, n\, \sigma_i\, N(t) \;-\; n_e / \tau_{ce} \;=\; 0 \qquad (28)$$

Since $\tau_{ce} << T_{inj}$, we have at the end of the injection process,

$$\chi \;=\; n_e / N_T \;=\; 1/2\ \beta\, c\, n\, \sigma_i\, \tau_{ce} \;=\; 0.002\, \tau_{ce} / T_{inj} \qquad (29)$$

that is a neutralization coefficient $\chi = 0.003$ %, comparable to what it is expected from the natural escape in the vertical direction. Thus it is not obvious that the use of the clearing electrodes in the NSNS Accumulator Ring could add any more beneficial effect.

The potential difference required between the pair of parallel clearing electrodes, assuming that they are separated by $2b = 20$ cm, during the passage of the beam bunch, is

$$U \;=\; 4\, N_T\, e\, b^2 / a^2\, L \;\sim\; 36\ \text{kVolt}, \qquad (30)$$

to be compared to only few Volts to sweep the electron away during the passage of the beam gap.

The e-p Instability

A coherent instability of the proton beam bunch can be triggered by the electromagnetic interaction with the cloud of electrons, when both beams have a finite displacement of the centers of mass that we shall denote Y_p and Y_e. To estimate the onset and the growth rate of the instability we shall neglect the longitudinal details of both beams, which we do not believe to be very important to the main features of the phenomenon. That is, we shall rely to the "coasting beam" theoretical model. The equations for Y_p and Y_e are then [1,3]

$$d^2Y_p / dt^2 \;+\; \Omega_\beta^2\, Y_p \;=\; (\chi\, r_p / \gamma\, r_e)\, \Omega_e^2\, (Y_e - Y_p) \qquad (31a)$$

$$d^2Y_e / dt^2 \;=\; \Omega_e^2\, (Y_p - Y_e) \qquad (31b)$$

where Ω_β is the angular betatron frequency, $r_p = 1.535 \times 10^{-18}$ m, and $r_e = 2.82 \times 10^{-15}$ m.

We shall look for a solution of the form

$$Y_p \;=\; \overline{Y}_p\ \exp i\,(k\theta - \Omega t) \qquad (32a)$$

$$Y_e \;=\; \overline{Y}_e\ \exp i\,(k\theta - \Omega t) \qquad (32b)$$

where Ω is an unknown collective angular frequency, which we expect to be a complex quantity, θ is the angular coordinate around the circumference of the ring, and k is a mode number which, of course, is expected to have only integer values. It is to be noticed that

$$d\, Y_p / dt \;=\; -i\,(\Omega - k\omega_0)\, Y_p \qquad (33a)$$

$$d\,Y_e / dt \quad = \quad -i\,\Omega\,Y_e \tag{33b}$$

where $\omega_0 = 2\pi f_0$. Substituting (32a and b) into the system of equations (31a and b), and requiring that the resulting determinant of the amplitudes $\overline{Y}_p$ and $\overline{Y}_e$ vanishes, give the following dispersion relation

$$1 \quad = \quad \Omega_p^2 / [\,(\Omega - k\omega_0)^2 \; - \; \Omega_\beta^2\,] \quad + \quad \Omega_e^2 / \Omega^2 \tag{34}$$

where

$$\Omega_p^2 \quad = \quad (\chi\, r_p / \gamma\, r_e\,)\, \Omega_e^2 \tag{35}$$

The dispersion relation (34) is then solved to derive Ω versus the mode number k. The growth rate of the instability is given by the imaginary part of Ω

The results for the NSNS Accumulator Ring are shown in Figures 15 - 17. Figure 15 gives the region of instability and the growth rate versus the mode number k for several values of the neutralization coefficient at the ring operating tune $\nu = 3.8$. Since many parameters are fairly uncertain, k was varied continuously to give a better idea of the range of unstable parameters. It is seen that with $\chi = 1\%$ one mode k = 75 is unstable. But if $\chi < 0.1\%$ the instability can be avoided. This is seen better in Figure 16 which assumes a neutralization coefficient $\chi = 0.01$ % and different values of the betatron tunes. By letting the betatron tune change between 3.7 and 3.9, the instability is always avoided. Figure 17 shows that even with $\chi = 0.1$ % the instability can be avoided by carefully tuning the ring.

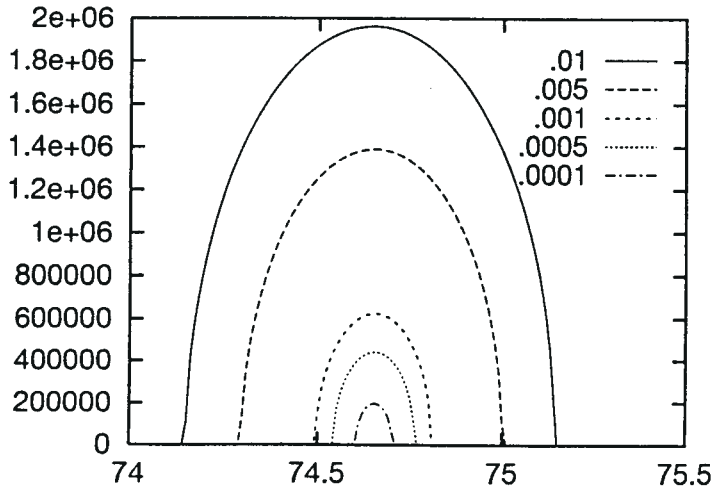

Figure 15. ep-Instability Growth Rate (1/s) vs. the Mode Number k
for several values of the Neutralization Coefficient χ.

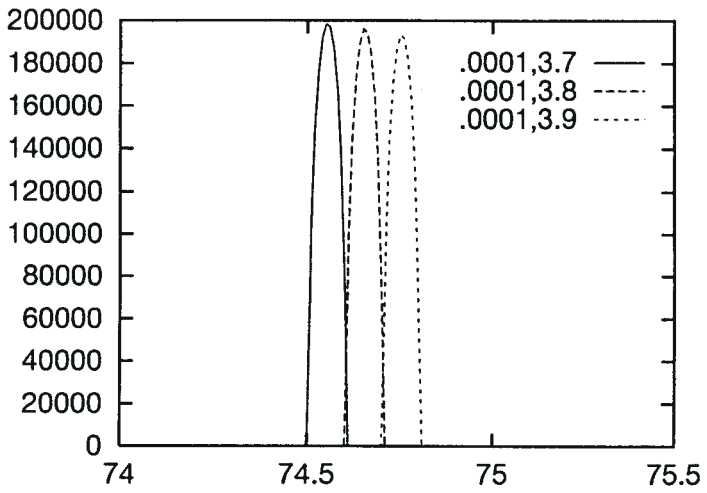

Figure 16. ep-Instability Growth Rate (1/s) vs. the Mode Number k for several values of the Ring Tunes and $\chi = 0.0001$.

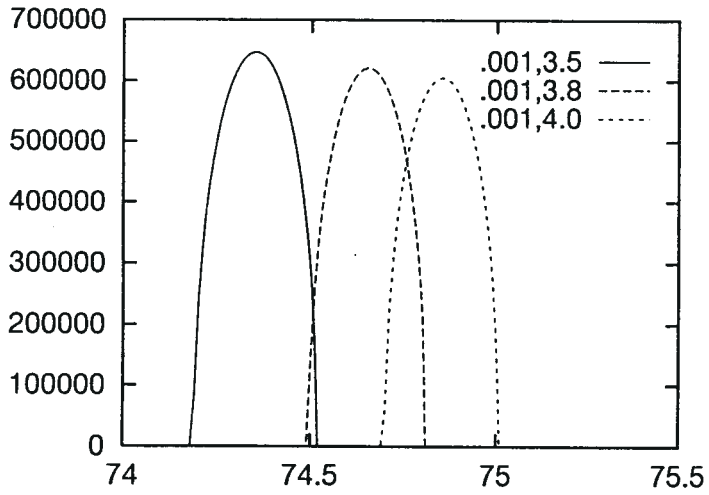

Figure 17. ep-Instability Growth Rate (1/s) vs. the Mode Number k for several values of the Ring Tunes and $\chi = 0.001$.

Conclusions

Though ion-induced instabilities have clearly been observed in electron storage rings, one can hardly explain the occurrence of electron-induced effects in rings with bunched proton beams. Once the role of the ions and electrons is inverted, because of the large difference in mass, the proton bunched beam is stable provided fundamental precautions are taken in the design of the ring, namely: a sufficiently large gap to give a chance to the electrons to escape, a good vacuum pres-

namely: a sufficiently large gap to give a chance to the electrons to escape, a good vacuum pressure of at least 10^{-9} mmHg, efficient compressing rf system which eliminates beam leakage into the gap to at least 10^{-3} level, and control of all possible electron sources in the ring. Finally, the material of the vacuum chamber is to be conveniently chosen to eliminate secondary electron emission.

To complete the present analysis there are still a number of peripheral issues which need to be investigated in the near future. They are: (1) Careful study of the motion of the electrons when they are only partially confined transversely within the proton beam dimension; (2) Detailed numerical study of the motion of the electrons in the quadrupole magnets; and (3) Evaluation of the e-p instability including the actual azimuthal dependence of both beams.

References

[1] T. Wang et al., Recent Study of Beam Stability in the PSR, Proceedings of the 1993 PAC, Washington, DC, May 1993. Volume 5 of 5, page3297.

[2] Y. Baconnier, Neutralization of Accelerator Beams by Ionization of the Residual Gas, Proccedings of the CERN Accelerator School, Gif-sur-Yvette, Paris, France. 3-14 September 1984. CERN 85-19, Vol. I, page 267.

[3] B.V. Chirikov, Stability of a Partially Compensated Electron Beam. Soviet Atomic Energy, Vol. 19, p 1149-1155 (1965).

[4] A comprehensive list of technical notes describing electron-induced effects in the ISR can be found in the review lecture of Y. Baconnier in reference [2].

[5] D. Neuffer et al., *Nucl. Instr. and Meth.* **A321**, 1 (1192).

[6] A.G. Ruggiero, L. Blumberg, Y.Y. Lee and A. Luccio, The NSNS Accumulator Ring. BNL/NSNS Technical Note No. 001. August 5, 1996.

[7] LANSCE Performance Improvements Phase II, LANL Proposal R-1339-95-0.

[8] L.N. Blumberg and Y.Y. Lee, H^- Charge Exchange Injection into the 1 GeV NSNS Accumulator. BNL/NSNS Technical Note No. 003. November 1, 1996.

[9] H. Ludewig, private communication, BNL, december 1996.

[10] F. Lapique and F. Piuz, *Nucl. Instr. and Meth* **175** (1980), p. 297-318.

[11] M. Blaskiewicz, J.M. Brennan and Y.Y. Lee, RF Options for the NSNS. BNL/NSNS Technical Note No. 009. December 5, 1996.

[12] A.U. Luccio, D. Maletic and F.W. Jones, Injection and RF Capture in the NSNS. BNL/NSNS Technical Note No. 004. December 5, 1996.